ELSEVIER

Journal of Power Sources 111 (2002) 121–129

JOURNAL OF POWER SOURCES

www.elsevier.com/locate/jpowsour

Study of molten carbonate fuel cell—microturbine hybrid power cycles

Francisco Jurado*

Department of Electrical Engineering, University of Jaén, 23700 EUP Linares (Jaén), Spain

Received 4 January 2002; accepted 8 May 2002

Abstract

The interaction realized by fuel cell—microturbine hybrids derive primarily from using the rejected thermal energy and combustion of residual fuel from a fuel cell in driving the gas turbine. This leveraging of thermal energy makes the high temperature molten carbonate fuel cells (MCFCs) ideal candidates for hybrid systems. Use of a recuperator contributes to thermal efficiency by transferring heat from the gas turbine exhaust to the fuel and air used in the system.

Traditional control design approaches, consider a fixed operating point in the hope that the resulting controller is robust enough to stabilize the system for different operating conditions. On the other hand, adaptive control incorporates the time-varying dynamical properties of the model (a new value of gas composition) and considers the disturbances acting at the plant (load power variation).

Keywords: Gas turbines; Molten carbonate fuel cell (MCFC); Power systems simulation

1. Introduction

Fuel cells are particularly well suited for power generation in co-generation plants because they convert energy directly into electricity in an electrochemical process while simultaneously producing heat [1–3]. However, it is first necessary to reform fuels such as natural gas, converting it into a gas with a high hydrogen content, so that it can be electrocatalytically oxidized with air.

The direct carbonate fuel cell is a variant of molten carbonate fuel cells (MCFCs) in that it internally reforms methane-containing fuels within the anode compartment of the fuel cell [4–7]. The largest demonstration of MCFC technology has been California's 2-MW Santa Clara Demonstration Project [8].

Microturbines, which are typically fueled with natural gas, generate between 25 and 200 kW of electricity. Their small size and relatively low cost allow them to be located near where they are needed. They can operate at very low emission levels and reduce the efficiency losses and environmental impact of large transmission and distribution systems. In this paper, a MCFC is associated with a gas microturbine to produce electric power.

Hybrid systems offer a solution to two important problems, the low efficiency and relatively high emissions of small gas turbines, and the high cost of small fuel cell power plants [9–11].

The paper is structured as follows. Section 2 presents a review of the MCFC. Some basic concepts of the gas turbine theory are presented in Section 3. Section 4 describes the gas turbine control configuration. Section 5 briefly discusses the fuel cell—microturbine hybrid power cycles. Section 6 outlines the adaptive control. Section 7 depicts some simulation results and discussion. Finally, conclusions are presented in Section 8.

2. Molten carbonate fuel cells

MCFC can reach fuel-to-electricity efficiencies approaching 60%, considerably higher than the 37–42% efficiencies of a phosphoric acid fuel cell (PAFC) plant. When the waste heat is captured and used, overall fuel efficiencies can be as high as 85%.

Improved efficiencies are one reason why MCFC offers significant cost reductions over PAFC technology. Another is that the electrodes of a MCFC be made of nickel catalysts rather than the more costly platinum of PAFC systems.

Natural gas is internally reformed, partially in an internal reforming unit and partially at the cells, eliminating the need

* Tel.: +34-53-026518; fax: +34-53-026508.
E-mail address: fjurado@ujaen.es (F. Jurado).

0378-7753/02/$ – see front matter
PII: S0378-7753(02)00340-3

Nomenclature

Fuel cell

E_0	standard potential
F	Faraday's constant
i	cell load current
P_i	partial pressure, $P_{i,a} = x_{ai}P_a/P_{atm}$, $P_{i,c} = x_{ci}P_c/P_{atm}$
V_c	cell voltage under load current
V_0	equilibrium potential
z	cell ohmic impedance
η_{act}	activation polarization
η_{conc}	concentration polarization

Gas turbine

a, b, c	valve parameters
c_{pa}	specific heat of air at constant pressure
c_{pg}	specific heat of combustion gases
c_{ps}	specific heat of steam
e_1	valve position
F_d	fuel demand signal
Δh_{IC}	isentropic enthalpy change for a compression from $p_{c_{in}}$ to $p_{c_{out}}$
Δh_{IT}	isentropic enthalpy change for a gas expansion from $p_{T_{in}}$ to $p_{T_{out}}$
Δh_{25}	specific enthalpy of reaction at reference temperature of 25 °C
HHV	higher heating value
k_f	fuel system gain constant
k_{HHV}	factor which depends on HHV
$p_{c_{in}}$	air pressure at compressor inlet
$p_{c_{out}}$	air pressure at compressor outlet
$p_{T_{in}}$	pressure of combustion gases at turbine inlet
$p_{T_{out}}$	pressure of combustion gases at turbine outlet
P_c	compressor power consumption
P_{mec}	mechanical power delivered by turbine
P_T	total mechanical power delivered by turbine
t	time
T	mechanical torque delivered by turbine
$T_{c_{out}}$	outlet air temperature
T_{is}	temperature of injected steam
$T_{T_{in}}$	turbine inlet gas temperature
w_a	air mass flow into the compressor
w_f	fuel mass flow
w_g	turbine gas mass flow
w_{is}	injection steam mass flow
η_c	overall compressor efficiency
η_{trans}	transmission efficiency from turbine to compressor
η_T	overall turbine efficiency
τ_f	fuel system time constant
ω	rotation speed of the turbine
$\Delta\omega$	rotation speed deviation of the turbine

Adaptive control

$A(z^{-1})$, $B(z^{-1})$	polynomials of the plant
$B_r^-(z^{-1})$, $B^-(z^{-1})$	polynomials of the performance index
$e(i)$	disturbance of the plant
h	constant term
ΔI_{dc}	stack current deviation
J	performance index
K	prediction horizon in the performance index
$P(z^{-1})$, $Q(z^{-1})$, $V(z^{-1})$	filter polynomials
$P_{\_init}$	covariance matrix
ΔP_L	load power variation
q	weighting coefficient
r_1, r_2	varying parameters of the polynomial $R_c(z^{-1})$
$R(z^{-1})$, $S(z^{-1})$, $T(z^{-1})$	polynomials of the difference equation
s_d	standard deviation
s_1, s_2	varying parameters of the polynomial $S_c(z^{-1})$
$S_c(z^{-1})$, $R_c(z^{-1})$	polynomials of the controller
$u(i)$	plant control signal
$y(i)$	plant output signal
λ	forgetting factor
σ^2	constant variance
$\omega(i)$	setpoint of the plant output signal

for a large external reforming unit to produce hydrogen fuel. The approach (Fig. 1) is a combination of indirect internal reforming (IIR) and direct internal reforming (DIR) which provides for better thermal management. At the cathode, oxygen reacts with carbon dioxide and electrons to form carbonate ions:

$$\tfrac{1}{2}O_2 + CO_2 + 2e^- \rightarrow {CO_3}^{2-} \quad (1)$$

The carbonate ions flow through the electrolyte matrix from cathode to anode. At the anode, the carbonate ions are consumed by the oxidation of hydrogen to form steam and carbon dioxide, releasing electrons to the external circuit:

$$H_2 + {CO_3}^{2-} \rightarrow H_2O + CO_2 + 2e^- \quad (2)$$

Cell voltage under load current (A/cm) is expressed as [12]:

$$V_c = V_0 - \eta_{act} - \eta_{conc} - iz \quad (3)$$

Activation polarization is caused by electrode kinetics while concentration polarization is caused by concentration gradients in the electrode. Equilibrium potential is described by the Nernst equation [12]:

$$V_0 = E_0 + \frac{RT}{2F}\ln\left(\frac{P_{H_2,a}P_{O_2,c}^{1/2}P_{CO_2,c}}{P_{H_2O,a}P_{CO_2,a}}\right) \quad (4)$$

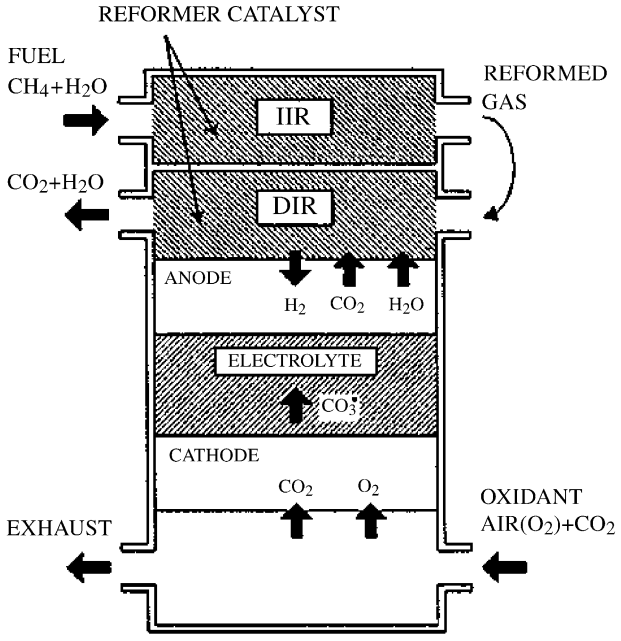

Fig. 1. IIR/DIR structure of MCFC stack.

Partial pressures (normalized to atmospheric pressure) depend on anode/cathode gas pressure and composition while standard potential and ohmic impedance are both temperature dependent. Fuel cell polarization losses are generally dependent on partial pressures, temperature and current density, and are spatially distributed in an actual cell. In this paper, the dynamic model is a lumped parameter, where outlet properties are equal to average properties [13–15].

3. Gas turbine

A thorough introduction to gas turbine theory is provided in the book of Cohen et al. [16]. There also exist a large literature on the modeling of gas turbines. Model complexity varies according to the intended application. Detailed first principle modeling based upon fundamental mass, momentum and energy balances is reported by Fawke et al. [17] and Shobeiri [18]. These models describe the spatially distributed nature of the gas flow dynamics by dividing the gas turbine into a number of sections. Throughout each section, the thermodynamic state is assumed to be constant with respect to the location, but varying with respect to time. Mathematically, the full partial differential equation model description is reduced to a set of ordinary differential equations, which facilitate easier application within a computer simulation program. For a detailed model, a section might consist of a single compressor or turbine stage. Much simpler models result if the gas turbine is decomposed into just three sections corresponding to the main turbine components, i.e. compressor, combustor and turbine [19].

Another modeling approach is by utilizing real steady-state engine performance data [20]. It is assumed that transient thermodynamic and flow processes are characterized by a continuous progression along the steady-state performance curves, this is known as the *quasi-static* assumption. The dynamics of the gas turbine, e.g. combustion delay, motor inertia, fuel pump lag, etc. are then represented as lumped quantities separate from the steady-state performance curves. Very simple models result if it is further assumed that the gas turbine is operated at all times close to rated speed [21].

In terms of energy conversion, chemical energy present in the combustion reactants is transferred to the gas stream during combustion. This energy—measured in terms of gas enthalpy or higher heating value (HHV)—is then converted into mechanical work, by expanding the gas through the turbine. Thus, the excess mechanical power available for application elsewhere, after accounting for the power required to drive the compressor is derived ultimately from the combustion process. Without combustion, assuming 100% efficient compressor and turbine operation, the power developed by the turbine would be exactly matched by the power required to drive the compressor.

Compressor power consumption equation:

$$P_c = \frac{w_a \Delta h_{IC}}{\eta_c \eta_{trans}} \tag{5}$$

Combustion energy equation:

$$w_g c_{pg}(T_{T_{in}} - 298) + w_f \Delta h_{25} + w_a c_{pa}(298 - T_{c_{out}}) + w_{is} c_{ps}(298 - T_{is}) = 0 \tag{6}$$

Power delivery equation:

$$P_T = \eta_T w_g \Delta h_{IT} \tag{7}$$

$$P_{mec} = P_T - P_c \tag{8}$$

Fig. 2 shows the block diagram of the gas turbine.

4. Gas turbine control configuration

The concept of the gas turbine control system, which is applied in this paper, is based on the Speedtronic Mark 4 description as presented in the paper by Rowen [22]. Some considerations concerning the subject may be also found in [23,24].

The simplified gas turbine model is divided into two interconnected subsystems in this paper. The subsystems are: the fuel system (fuel valve with actuator), and the turbine.

The fuel system consists of the fuel valve and the actuator. The fuel flow out from the fuel systems result from the inertia of the fuel system actuator and of the valve positioner.

Fuel system actuator equation:

$$w_f = \frac{k_f}{\tau_f s + 1} e_1 \tag{9}$$

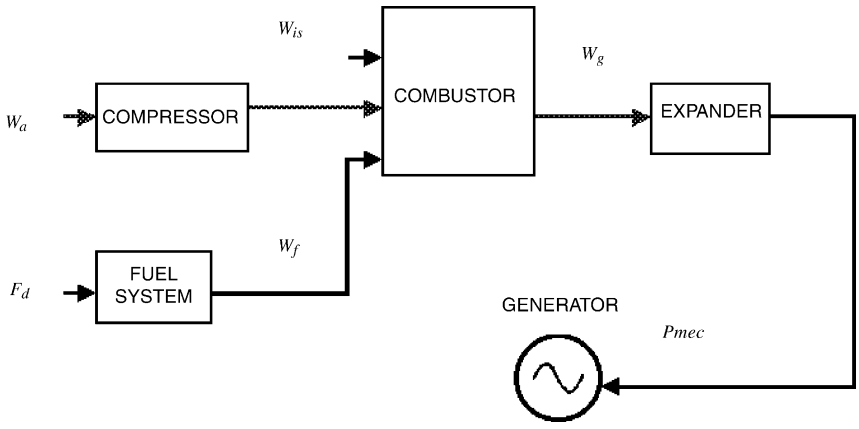

Fig. 2. Gas turbine.

Valve positioner equation:

$$e_1 = \frac{a}{bs + c} F_{\mathrm{d}} \tag{10}$$

Input variable to the fuel system is F_{d}. Output variable from the fuel system model is w_{f}.

A single gas turbine does not require the digital setpoint feature. The turbine torque function is given by:

$$T = k_{\mathrm{HHV}}(w_{\mathrm{f}} - 0.23) + 0.5(\Delta\omega) \tag{11}$$

The k_{HHV} and 0.23 factors cater for the typical turbine power/fuel rate characteristic, which rises linearly from zero power at 23% fuel rate to rated output at 100% fuel rate.

The Eq. (11) allows the turbine torque to be calculated algebraically. This torque is used in the equations which model the mechanical system:

$$P_{\mathrm{mec}} = T\omega \tag{12}$$

Input variables to the turbine are w_{f}, $\Delta\omega$ and ω. Output variable from the turbine is P_{mec}.

For the purpose of this paper, only modulating control of mechanical side of the gas turbine is of interest. The simplified model of the gas turbine controller in this paper consists of two inputs and one output. Inputs to the controller are P_{mec} and ω. Output from the controllers is F_{d}.

The block diagram of the gas turbine control system is presented in Fig. 3. The diagram consists of two PID controllers. LVG stands for least value gate that transmits the minimum of two incoming signals.

5. Fuel cell/turbine hybrid

When used in combination with turbines, fuel cells can produce from 55 to 90% of the electricity of the system while turbines produce the remainder [10]. Several cycle configurations have been proposed and the terminology is still evolving, but one useful way of looking at the differences is to divide the configurations into those that include "directly fired turbines" and those with "indirectly fired turbines". A hybrid power system with a "directly fired turbine" normally uses a pressurized fuel cell to provide input to the turbine, thus, acting as a combustor. In the "indirectly fired turbine" system an atmospheric fuel cell is

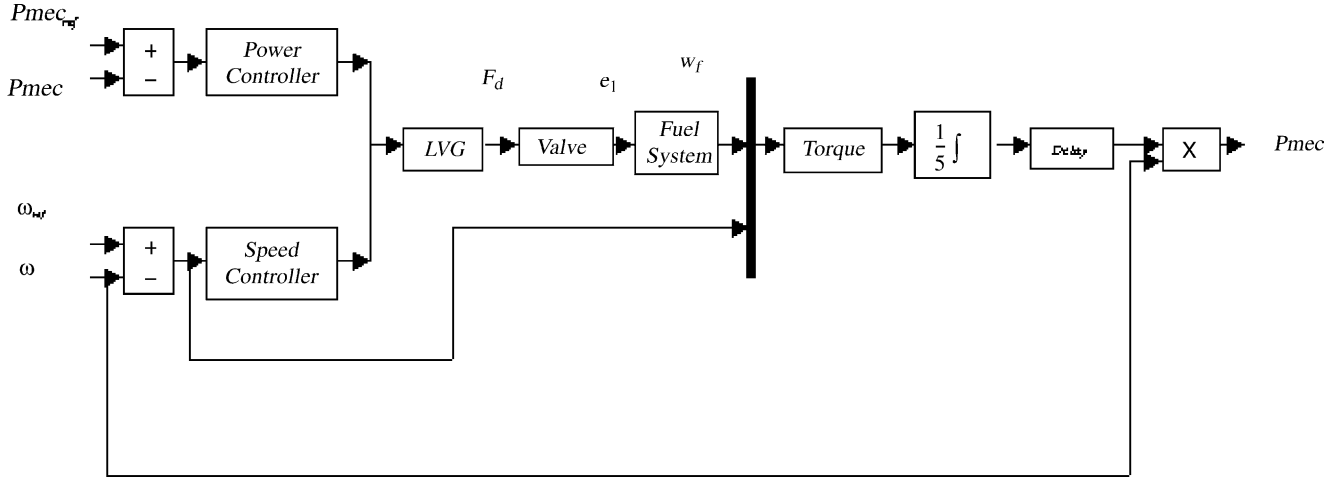

Fig. 3. Gas turbine control system.

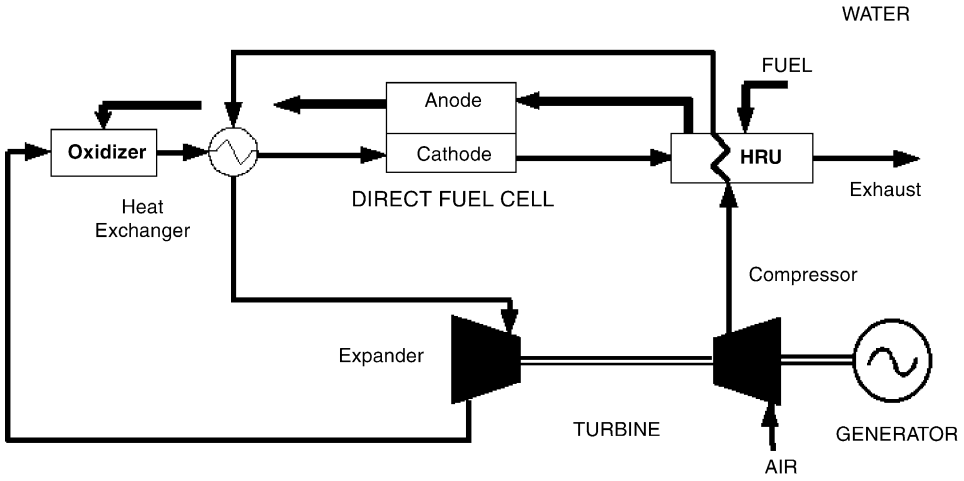

Fig. 4. Fuel cell/turbine hybrid system.

used and a pressurized heat exchanger provides input to the turbine. When utilizing the fuel cell/gas turbine combination the combined efficiency of the system is raised to >60% and criteria pollutant emissions are essentially eliminated.

An example of a hybrid system with an ''indirectly fired turbine'' is shown in Fig. 4. This type of integration could utilize any gas turbine system. The indirectly fired approach posits the fuel cell in the exhaust of an indirectly fired gas turbine. The air and residual products of the fuel cell are then fed to an atmospheric combustor. This combustor heats the air leaving the compressor via a heat recovery unit (HRU) and delivers it to the turbine. The combination of the atmospheric combustor and heat exchanger replaces the normal internal pressurized combustor.

The turbine exhaust flows to the fuel cell anode exhaust oxidizer. Exhaust from the anode exhaust oxidizer flows to the heat exchanger, which provides the heat for the compressor air. The exit from the heat exchanger flows through the fuel cell cathode providing the oxygen and carbon dioxide needed in the carbonate fuel cell process.

In the ''indirectly fired turbine'' system, the fuel cell does not need to operate at the turbine pressure, instead it operates at the preferred ambient pressure and is independent of gas turbine cycle pressure ratio. The system works efficiently with a wide range of turbine compression ratio. This allows taking a system developed for integration at the multi-MW scale with industrial size turbines, and configuring a small MW class system using a microturbine at a lower pressure ratio.

6. Adaptive control

A real-world plant can be usually characterized by time-varying dynamical properties, which affect the plant behavior. Stochastic models are used to represent the disturbances acting at the plant output because of the large number and different nature of the factors disturbing the normal plant operation.

Robustness properties can usually be ensured by the feedback structure of the control system. The feedback compensates for the deviation of the plant output signal value from its setpoint: disturbances affecting the plant (load power variation) or change in the plant model parameters (HHV), such a change, is convenient to observe parameter tracking.

It may be possible to identify the parameters of the controller that we are seeking. This scheme is called direct adaptive control, because we are going to obtain directly the required controller parameters through their estimation in an appropriately redefined plant model.

Adaptive control is usually used to cope with an unknown or/and changing plant to be controlled [25]. Analysis and synthesis of such a control system is possible only under some assumptions concerning the nature of the plant and its dynamics. In this paper, only linear, discrete-time plants disturbed in a stochastic manner will be considered. The following plant model will be used [26]:

$$y(i) = z^{-k}\frac{B(z^{-1})}{A(z^{-1})}u(i) + e(i) \tag{13}$$

Eq. (13) is one of the most typical in the field of adaptive control and non-standard discrete-time control algorithms in general. If only stable factors exist in the B polynomial, the plant will be called minimum phase. The part $e(i)$ is the stochastic part of the disturbance. In this paper, this disturbance is the load power variation ΔP_L.

Generally, most control algorithms can be described by the structure and parameters of the difference equation [26]:

$$R(z^{-1})u(i) + S(z^{-1})y(i) - T(z^{-1})\omega(i) + h = 0 \tag{14}$$

The coefficients of the $R(z^{-1})$, $S(z^{-1})$ and $T(z^{-1})$ polynomials and the h term are chosen before the simulation experiment and stay constant during the experiment.

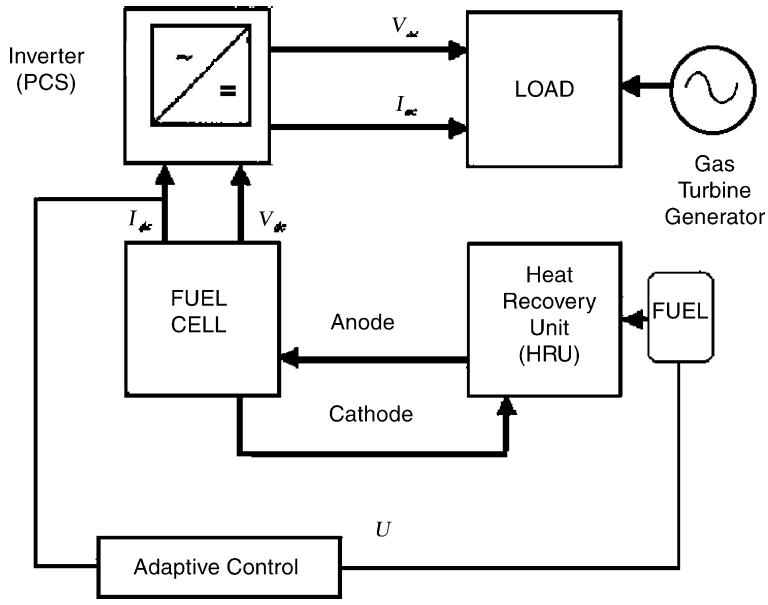

Fig. 5. Fuel cell control system.

The aim of the minimum variance control algorithm is the minimization of the following performance index [25,27]:

$$J = E\left\{\left[P(z^{-1})\frac{B_r^{-}(z^{-1})}{B^{-}(z^{-1})}y(i+K) - V(z^{-1})\omega(i)\right]^2 + q[Q(z^{-1})u(i)^2]\right\} \quad (15)$$

where $B_r^{-}(z^{-1})$ is the reciprocal polynomial of the $B^{-}(z^{-1})$ polynomial. Minimization of this performance index leads to a control algorithm of the same structure as Eq. (14).

The estimation scheme used in this paper is the recursive least squares (RLS). The adaptive control is shown in Fig. 5. Stack current I_{dc} is measured and used in calculation of fuel flow setpoint. This measurement of the stack current determines the plant output signal $y(i)$. Stack current is continuously adjusted by the inverter control to maintain power. This current is the setpoint of the plant output signal $\omega(i)$.

7. Results and discussion

A plant consisting of a load is fed from the fuel cell/turbine hybrid system. The selected system comprises a 250 kW fuel cell and a 30 kW gas microturbine. The plant and the fuel cell/microturbine system are modeled using MATLAB™.

All parameters correspond to a two-stack equivalent. The fuel cell stacks used in this paper are rated at 125 kW. Stack voltage is taken across a parallel connection of two stacks, each stack consisting of 258 cells.

To investigate transient behavior, the plant is assumed to be at steady-state corresponding to rated power and subjected to a sudden variation in power demand. The HRU, power conditioning system (PCS), and plant control system are included in the simulation [28–31]. The inverter is assumed to regulate load voltage perfectly, and simply draws stack current proportional to load current and inversely proportional to stack voltage using a power demand setpoint. The time constants for changes in power output for the microturbines and fuel cell range from 5 ms to 50 s, and the PCS dynamics are not important [32].

This paper develops the control system with an adaptive minimum variance controller. The plant and the controller are simulated as discrete in time [33]. The plant parameters are: polynomials $A(z^{-1})$, $B(z^{-1})$ and standard deviation s_d of white noise of normal distribution. Parameters of RLS are: initial values of diagonal of covariance matrix $P_{\_init}$ and forgetting factor λ.

The disturbance considered is a load power variation ΔP_L. This is zero-mean, white noise and has constant variance σ^2.

The controller has the form [27]:

$$u(i) = -\frac{S_c(z^{-1})}{R_c(z^{-1})}y(i) \quad (16)$$

where S_c and R_c are of order 2. The structure of the controller is calculated according to the plant structure. To show the ability of the controller to adapt to varying operating conditions, a new value of gas composition is introduced at 100 s what provides time-varying plant. Controller parameters are identified on-line and the simulation time is 200 s.

The minimum variance controller serves as an example of a self-tuner. The optimal value of the output signal standard deviation is obtained in the steady-state. The plant is assumed to be of Auto Regressive with eXogenous input (ARX) type.

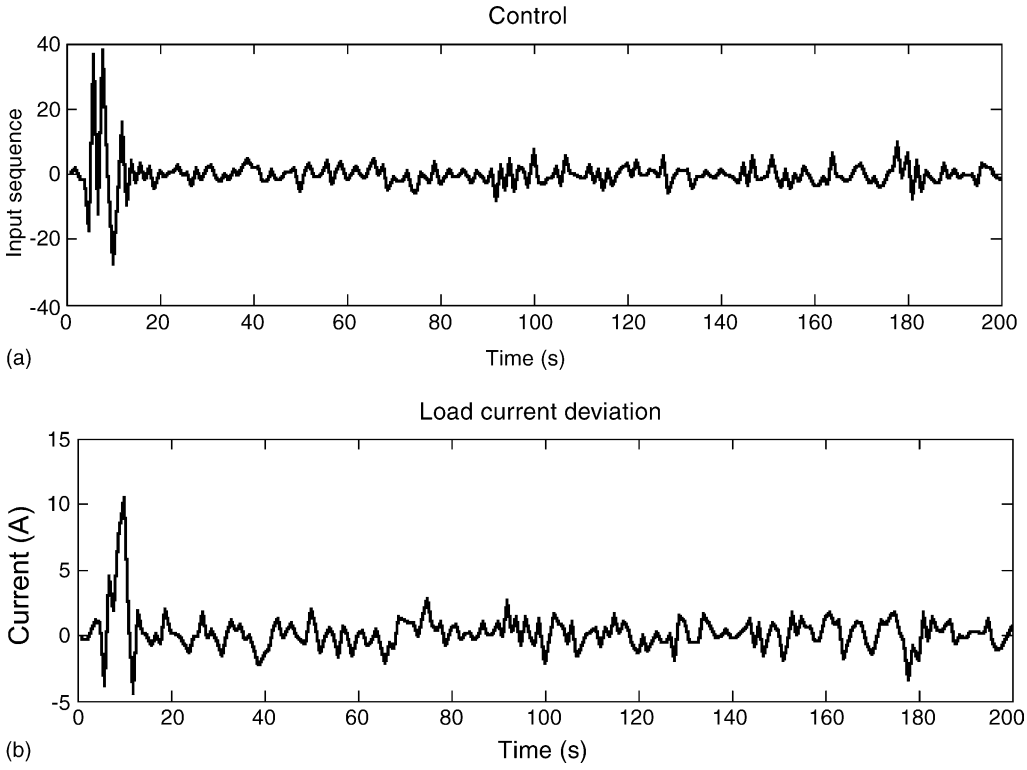

Fig. 6. (a) Control signal U; (b) load current deviation ΔI_{dc}.

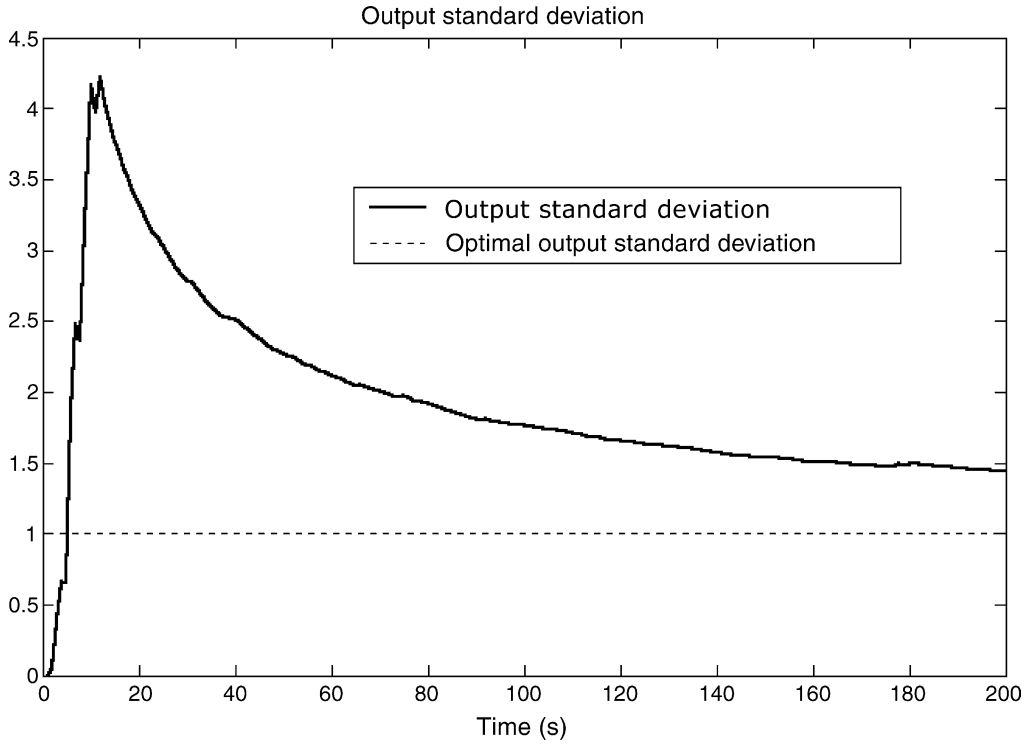

Fig. 7. Output standard deviation s_d and the optimal output standard deviation.

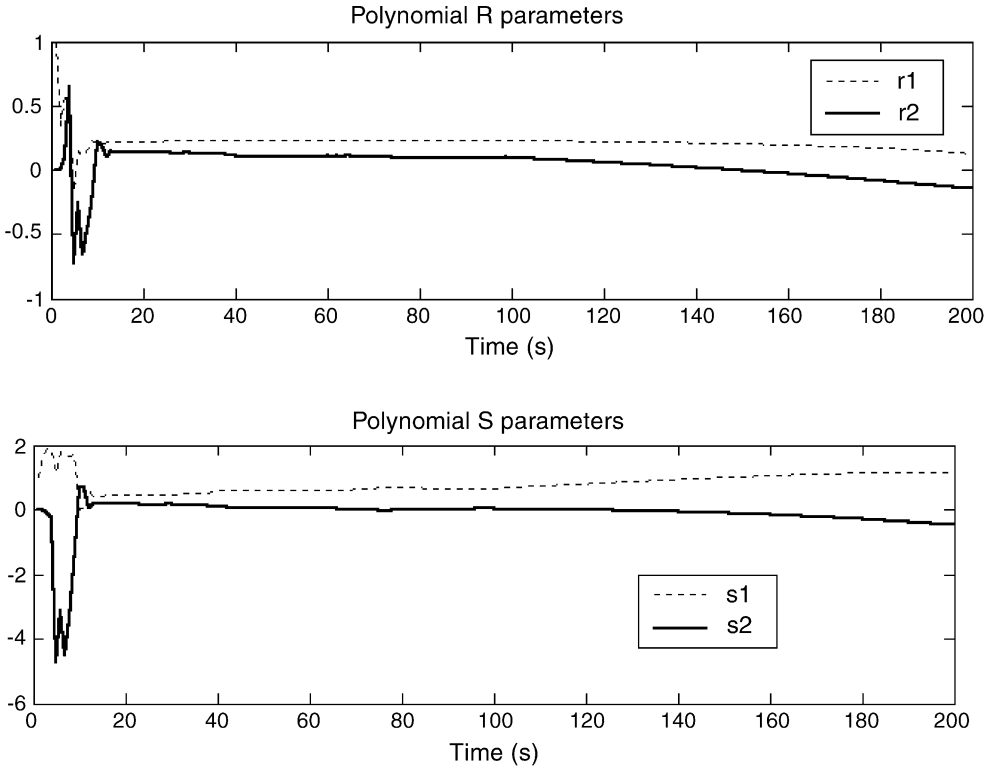

Fig. 8. (a) Polynomial R parameters (r_1, r_2); (b) polynomial S parameters (s_1, s_2).

The results with the derived model are summarized. Fig. 6a presents the control signal U. Referring to the results shown in Fig. 6b, it can be seen the stack current deviation ΔI_{dc}. Stack voltage starts at its initial value, corresponding to regulated power, and drops quickly to a sudden increase in stack current, in turn, controlled by the inverter to maintain the new power setpoint. Stack voltage varies according to the temperature dependence, while stack current is continuously adjusted by the inverter control to maintain power.

Fig. 7 shows the output standard deviation s_d and the optimal output standard deviation. Fig. 8a depicts the polynomial R parameters where the varying parameters considered are r_1 and r_2. Fig. 8b displays the polynomial S parameters, s_1 and s_2 being the varying parameters. This controller guarantees some additional robustness margins in the case that the model does not cover the entire plant uncertainty.

8. Conclusion

The emerging fuel cells produce very high temperature exhaust gases that can be used to drive a gas turbine. A dynamic model for this MCFC—microturbine system has been elaborated.

A MCFC stack interacts with other system components and causes an interdependency between them. To investigate transient behavior, the plant is assumed to be at steady-state corresponding to rated power and subjected to a sudden variation in power demand. This paper develops the control system with an adaptive minimum variance controller and based on the simulation study, the resulting controller is robust enough to stabilize the system for different operating conditions.

References

[1] J.L. Silveira, E.M. Leal, L.F. Ragonha, Analysis of a molten carbonate fuel cell: cogeneration to produce electricity and cold water, Energy 26 (10) (2001) 891–904.
[2] M. Akai, N. Nomura, H. Waku, M. Inoue, Life-cycle analysis of a fossil-fuel power plant with CO_2 recovery and a sequestering system, Energy 22 (2/3) (1997) 249–255.
[3] E.M. Leal, J.L. Silveira, Study of fuel cell cogeneration systems applied to a dairy industry. J. Power Sources 16 (2002) 102–108.
[4] S. Matsumoto, A. Sasaki, H. Urushibata, T. Tanaka, Performance model of molten carbonate fuel cell, IEEE Trans. Energy Conv. 5 (2) (1990) 252–258.
[5] M. Farooque, Development of internal reforming carbonate fuel cell technology, final report, prepared for US DOE/METC, DOE/MC/23 274-2941, 1991, Chapter 3, pp. 6–11.
[6] A. Sasaki, S. Matsumoto, M. Fujitsuka, T. Shinoki, T. Tanaka, J. Ohtsuki, CO_2 recovery in molten carbonate fuel cell system by pressure swing adsorption, IEEE Trans. Energy Conv. 8 (1) (1993) 26–32.
[7] T. Shinoki, M. Matsumura, A. Sasaki, Development of an internal reforming molten carbonate fuel cell stack, IEEE Trans. Energy Conv. 10 (4) (1995) 722–729.
[8] Fuel Cell Engineering Corporation, 2 MW Fuel cell demonstration power plant test report, TR-108 252, prepared for EPRI, Santa Clara, July 1997.

[9] G. Steinfeld, H.C. Maru, R.A. Sanderson, High efficiency carbonate fuel cell/turbine hybrid power cycles. IECEC 96, in: Proceedings of the 31st Intersociety Energy Conversion Engineering Conference, Vol. 2, pp. 1123–1127. 11–16 Aug. 1996, Washington, DC, USA.

[10] A. Layne, N. Holcombe, National Energy Technology Laboratory, Fuel cell/gas turbine hybrid power systems for distributed generation: a status report, Global Gas Turbine News 2 (2000).

[11] H. Ghezel-Ayagh, A.J. Leo, H.C. Maru, Direct Fuelcell®/Turbine Hybrid System For Ultra High Efficiency Power Generation, Fuel Cell Energy Inc., 2002, Danbury, CT, USA.

[12] J.H. Hirschenhofer, D.B. Stauffer, R.R. Engleman, M.G. Klett, Fuel Cell Handbook, US Department of Energy, 1998, Washington, DC, USA.

[13] J. Ding, P.S. Patel, M. Farooque, H.C. Maru, A computer model for direct carbonate fuel cells, in: Proceedings of the Fourth International Symposium on Carbonate Fuel Cell Technology, Montreal, Que., 1997.

[14] M.D. Lukas, K.Y. Lee, H. Ghezel-Ayagh, Development of a stack simulation model for control study on direct reforming molten carbonate fuel cell power plant, IEEE Trans. Energy Conv. 14 (4) (1999) 1651–1657.

[15] M.D. Lukas, K.Y. Lee, H. Ghezel-Ayagh, An explicit dynamic model for direct reforming carbonate fuel cell stack, IEEE Trans. Energy Conv. 16 (3) (2001) 289–295.

[16] H. Cohen, G.F.C. Rogers, H.I.H. Saravanamuttoo, Gas Turbine Theory, 3rd Edition, Longman, New York, 1987.

[17] A.J. Fawke, H.I.H. Saravanamuttoo, M. Holmes, Experimental verification of a digital computer simulation method for predicting gas turbine dynamic behavior, Inst. Mech. Eng. Proc. 186 (1987) 27.

[18] T. Shobeiri, Digital computer simulation of the dynamic operating behaviour of gas turbines, Brown Boveri Rev. 3 (1987).

[19] A. Hussain, H. Seifi, Dynamic modeling of a single shaft gas turbine, in: Proceedings of the IFAC Symposium on Control of Power Plants and Power Systems, Munich, Germany, Pergamon Press, Oxford, 1992, pp. 43–48.

[20] W.W. Hung, Dynamic simulation of gas-turbine generating unit, IEE Proc. C 138 (1991) 4.

[21] W.J. Rowen, Simplified mathematical representations of heavy duty gas turbines, ASME J. Eng. Power 83-GT-63 (1983) 865–869.

[22] W.J. Rowen, Speedtronic Mark IV control system, Alsthom Gas Turbine Reference Library, AGTR 880, 1988.

[23] L.N. Hannett, A. Khan, Combustion turbine dynamic model validation from tests, IEEE Trans. Power Syst. 8 (1) (1993) 152–158.

[24] L.N. Hannett, G. Jee, B. Fardanesh, A governor/turbine model for a twin-shaft combustion turbine, IEEE Trans. Power Syst. 10 (1) (1995) 133–140.

[25] K.J. Aström, B. Wittenmark, Adaptive Control, 2nd Edition, Addison-Wesley, Reading, MA, 1995.

[26] J. Moscinski, Z. Ogonowski, Advanced Control with MATLAB™ and Simulink, Ellis Horwood, London, 1995.

[27] K.J. Aström, B. Wittenmark, Computer-Controlled Systems: Theory and Design, 2nd Edition, Prentice-Hall, Englewood Cliffs, NJ, 1990.

[28] Working Group on Prime Mover and Energy Supply Models, Dynamic models for combined cycle plants in power system studies, IEEE Trans. Power Syst. 9 (3) (1994) 1698–1708.

[29] L.N. Hannett, J.W. Feltes, Testing and model validation for combined-cycle power plants, in: Proceedings of the Power Engineering Society Winter Meeting, Columbus, OH, 2001, pp. 664–670.

[30] L.M. Tolbert, F.Z. Peng, T.G. Habetler, Multilevel converters for large electric drives, IEEE Trans. Ind. Appl. 35 (1) (1999) 36–44.

[31] M.D. Lukas, K.Y. Lee, H. Ghezel-Ayagh, Operation and control of direct reforming fuel cell power plant, in: Proceedings of the IEEE Power Engineering Society Winter Meeting, Vol. 1, Singapore, 23–27 January 2000, pp. 523–527.

[32] R. Lasseter, Dynamic models for micro-turbines and fuel cells, in: Proceedings of the PES Summer Meeting, Vol. 2, Vancouver, Canada, 15–19 July 2001, pp. 761–766.

[33] C.L. Phillips, H.T. Nagle, Digital Control System: Analysis and Design, 3rd Edition, Prentice-Hall, Englewood Cliffs, NJ, 1995.